Progress In Electromagnetics Research, PIER 99, 211–224, 2009

STUDY STAP ALGORITHM ON INTERFERENCE TARGET DETECT UNDER NONHOMOGENOUS ENVIRONMENT

Q.-Y. Gong and Z.-D. Zhu

Nanjing University of Aeronautics & Astronautics
Nanjing 210016, China

Abstract—In conventional statistical STAP algorithms, the existence of interference target in training samples will lead to signal cancellation, resulting in the output SCR falling and the moving target detection performance degrading. The nonhomogeneity detector is an effective way to restrain the outlier, which can improve the covariance matrix estimation by detecting the samples containing outliers and rejecting them, and improve the STAP performance. A new interference target detection algorithm is proposed in this paper, the outlier detection is realized by using the samples' data phase information. Compared with traditional method, the improved algorithm is more sensitive to interfering target with different azimuth and intensity. Simulation results demonstrate the validity of this improved method.

1. INTRODUCTION

Airborne radar systems are required to detect slow moving targets in the presence of both clutter and jamming. The ground clutter observed by an airborne radar platform is extended in both range and angle; it also spreads over a region in Doppler due to platform motion. A potential target may be obscured not only by mainlobe clutter that originates from the same angle as the target but also by sidelobe clutter that comes from a different angle but has the same Doppler frequency. The effect of sidelobe clutter may be eliminated with low-enough antenna sidelobes on transmitting and receiving. Many techniques have been developed for transmitting and receiving beams to accumulate target energy and reject clutter plus interference [1–8]. Although pattern synthesis can choose the antenna parameters to

Corresponding author: Q.-Y. Gong (gqy_lover@163.com).

obtain desired radiation characteristics, such as the specific position of the nulls, the desired sidelobe level and beamwidth of antenna pattern, most of these methods optimize only one parameter and have high computational complexity. Moreover, achieving very low-sidelobes in practice can be quite difficult, especially in the complex electromagnetic environment, and very expensive.

Space-Time Adaptive Processing (STAP) refers to the simultaneous processing of the spatial samples from an array antenna, and the temporal samples provided by the echoes form multiple pulses of a radar coherent processing interval (CPI). It is a candidate technology to improve the detecting and tracking of slow moving targets in difficult clutter and jamming environments [9–22]. STAP performance is determined in part by how closely its interference covariance matrix, typically estimated from adjacent range cells located symmetrically around the test cell, matches the interference statistics of the test range bin. The existence of interference target in training data will lead to mismatch of the interference covariance matrix estimation, resulting in the degrading of moving target detection performance. To minimize the loss in performance due to the outlier, a nonhomogeneity detector (NHD) was proposed to identify secondary data cells that contain outlier [11]; these data samples are then excised from the covariance matrix estimation. The generalized inner product (GIP) algorithm was used to process the measured data obtained from the Multi-Channel Airborne Radar Measurements (MCARAM) [12] program; the results show that 7 dB improvements in STAP processing when the outliers were discarded [13]. Therefore, the NHD is an effective method used to improve STAP performance under nonhomogenous environment. The main NHD include GIP [11], sample matrix inversion (SMI) [11], correlation dimension (CD) [14] and reiterative censoring adaptive power reside (RCAPR) [15–18], etc.

The existence of strong interference target in training samples will lead to the NHD algorithms such as GIP, SMI, and APR performance is severely degraded, resulting in the weaker ones cannot be detected and rejected [19]. The RCAPR algorithm has been shown to provide excellent detection performance in nonhomogeneous interference environments, but it has high computational complexity. Considering that the GIP detection result is not affected by the detect vector, it does not need to re-choice the training samples when the detection vector is changed, which significantly reduces the high computational complexity. Moreover, GIP can recognize the sidelobe interference target. In order to fully inherit the GIP's merit and overcome its shortcoming simultaneously, a new interfering target detection algorithm is developed, which applies samples data

phase information to screen training data for outliers. The improved algorithm performs outstanding operation, whether interference target exists or not. It is more sensitive to interfering target with different azimuth and intensity, more robust than GIP in selecting training data corrupted by multiple strong outliers.

2. STAP FUNDAMENTALS

2.1. Array Geometry

Figure 1 shows the geometry of an airborne array radar. "×" on a horizontal axis denotes the antenna element. The radar platform moves in the x-direction. We further define the x-direction as zero azimuth. θ denotes the azimuth, φ_l the depression angle, R_l the slant range, and v the platform velocity.

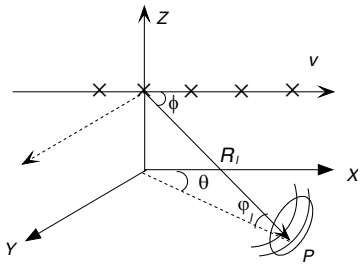

Figure 1. Geometry of airborne antenna arrays.

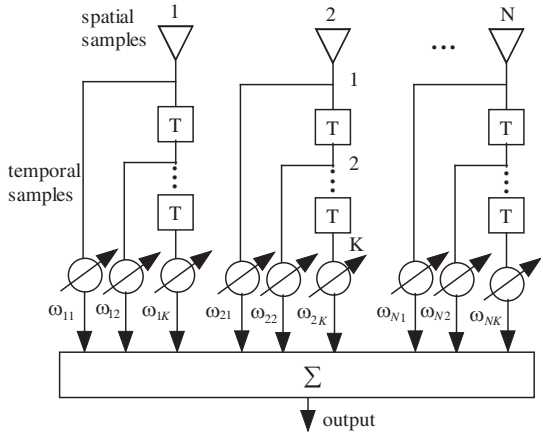

Figure 2. STAP architecture.

2.2. Data Models

Consider an N-element uniform linear array with interelement spacing d. The radar transmits an K-pulse waveform at pulse repetition interval T. The received data for each range gate may be arranged into a $NK \times 1$ space-time snapshot X_l formed by stacking the spatial snapshots from each pulse. A block diagram of the STAP is depicted in Figure 2. The data is processed at one range gate of interest, as depicted in Figure 3, which corresponds to one slice of the CPI data cube. Under the signal-presence hypothesis H_1

$$X_l = \alpha S(f_s, f_d) + X_c + X_j + X_n \tag{1}$$

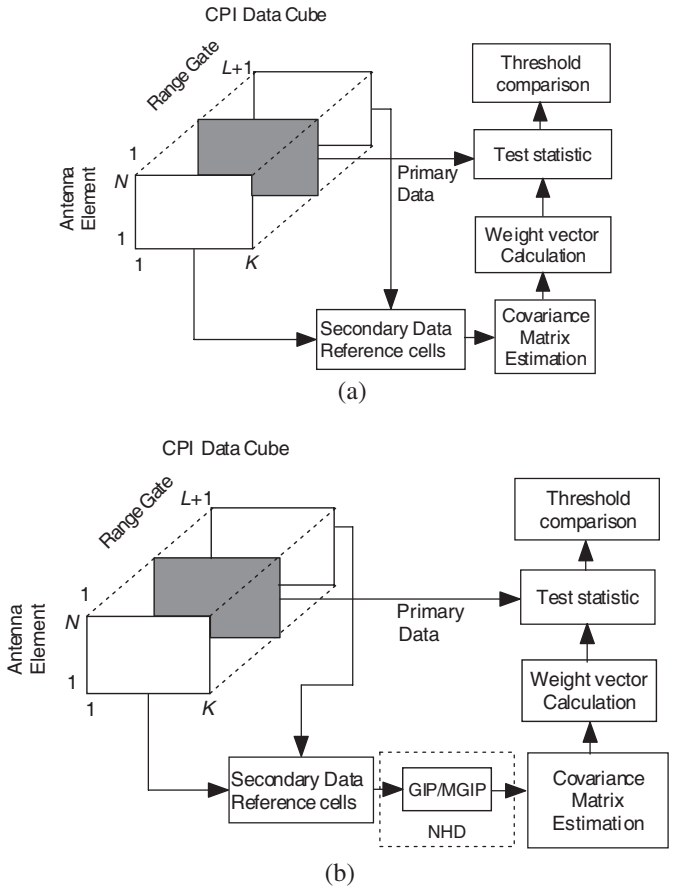

Figure 3. (a) the classical STAP data cube processing. (b) the STAP data cube processing with NHD.

here α is the target complex magnitude; $f_s = \frac{d}{\lambda}\cos\theta\cos\varphi_l, f_d = \frac{2v}{\lambda}\cos\theta\cos\varphi_l$ are the normalized spatial frequency and Doppler frequency respectively; X_c, X_j and X_n represent the ground clutter, jammers, and white noise. The $NK \times 1$ space-time steering vector S is given as follows

$$S(f_s, f_d) = S_t(f_d) \otimes S_s(f_s) \tag{2}$$

where, "$\otimes$" represents the Kronecker product; $S_s(f_s)$ and $S_t(f_d)$ are the spatial and time steering vectors

$$S_t(f_d) = \left[\begin{array}{cccc} 1 & e^{j\frac{2\pi f_d}{f_r}} & \cdots & e^{j(K-1)\frac{2\pi f_d}{f_r}} \end{array}\right]^T \tag{3}$$

$$S_s(f_s) = \left[\begin{array}{cccc} 1 & e^{j2\pi f_s} & \cdots & e^{j(N-1)2\pi f_s} \end{array}\right]^T \tag{4}$$

here, f_r denotes the pulse repetition frequency, $f_r = 1/T$.

The output of the space-time adaptive processor is

$$y_l = W_l^H X_l \tag{5}$$

where $W_l = [\omega_{11}\ \omega_{21}\ \ldots\ \omega_{N1}\ \ldots\ \omega_{1K}\ \omega_{2K}\ \ldots\ \omega_{NK}]^T$ is the adaptive weight vector and determined as follows

$$W_l = \hat{R}_l^{-1} S \tag{6}$$

here $\hat{R}_l$ is the covariance matrix estimated by secondary data chosen from range cells close to the cell under test. A fundamental issue, evident from (6), concerns accurately estimating the true, unknown covariance matrix. We typically estimate the covariance matrix via the minimum mean squared error (MMSE) as,

$$\hat{R}_l = \frac{1}{L}\sum_{k=l-L/2}^{k=l+L/2} X_k X_k^H, \quad k \neq l \tag{7}$$

3. THE INTERFERENCE TARGET DETECTION ALGORITHM

The underlying theory forming the basis of STAP for radar is based on the assumption that the noise and clutter field are stationary as well as independently and identically distributed (i.i.d) from range sample to range sample. The interference target existing in the secondary data violates the i.i.d assumption required to accurately compute the unknown covariance matrix via (7), resulting in degraded performance of the adaptive processor compared to theoretical predictions. In order to address this problem, a nonhomogeneous detector has been

devised for detecting which data are nonhomogeneous with respect to the majority and removing them from the STAP training data in Figure 3(b).

The GIP [11] test statistics is

$$\eta_{\mathrm{GIP}}\left(X_l, \hat{R}_L\right) = X_l^H \hat{R}_L^{-1} X_l \tag{8}$$

where X_l is the training sample, and $\hat{R}_L$ is a covariance matrix via the minimum mean squared error (MMSE) estimated by L secondary data. Define the whitening filter output as the $NK \times 1$ vector $\tilde{X}_l = \hat{R}_L^{-1/2} X_l$. Next, observe that (8) can be written as the inner product,

$$\eta_{\mathrm{GIP}}\left(X_l, \hat{R}_L\right) = \tilde{X}_l^H \tilde{X}_l \tag{9}$$

which equals the sum of the squares of $\tilde{X}_l$. The covariance matrix of $\tilde{X}_l$ is given as

$$\tilde{R}_l = E(\tilde{X}_l \tilde{X}_l^H) = E\left[\hat{R}_L^{-1/2} X_l X_l^H \hat{R}_L^{-1/2}\right] = \hat{R}_L^{-1/2} R_l \hat{R}_L^{-1/2} \tag{10}$$

where $R_l = E\left[X_l X_l^H\right]$ is the true covariance matrix of X_l. The expected value of η_{GIP} is

$$E(\eta_{\mathrm{GIP}}) = \mathrm{trace}\left(\tilde{R}_l\right) = \mathrm{trace}\left(\hat{R}_L^{-1/2} R_l \hat{R}_L^{-1/2}\right) \tag{11}$$

we regard signal vectors with similar values of η_{GIP} as homogeneous snapshots. A signal vector with η_{GIP} significantly varying from the mean is nonhomogeneous snapshot. While the GIP works well for clutter heterogeneity, it suffers from problems in dense target environments. For GIP test directly assesses both amplitude and phase information critical to defining covariance structure, the existence of strong target-like interferer in training samples will lead to signal cancelation, resulting in that GIP cannot distinguish the weaker ones from training samples. Aiming at resolving this problem, a new interference detection algorithm named as MGIP is proposed in this paper, which uses the samples' data phase information to reject the samples containing outlier. The algorithm is carried out as follows

$$\eta_{\mathrm{GIP}} = X_l^H \hat{R}_{pL}^{-1} X_l \tag{12}$$

where, $\hat{R}_{pL} = \frac{1}{L} \sum X_{pl}^T X_{pl}$, $X_{pl} = \arg(X_l)$, arg() denotes the phase of sample data; T denotes the transposition. It can prove that

$$E(\eta_{\mathrm{MGIP}}) = trace\left[\hat{R}_{pL}^{-1/2} R_l \hat{R}_{pL}^{-1/2}\right] \tag{13}$$

the sample vectors with η_{MGIP} significantly varying from the mean is nonhomogeneous. The MGIP algorithm has two merits as follows

1) MGIP algorithm can detect the weak interference target with the same Doppler frequency and azimuth as the strong one's. In GIP algorithm, the covariance matrix $\hat{R}_L$ is estimated directly by training data X_l. The existence of strong interference target will nullify in this direction and lead to signal cancelation, so the weaker one cannot be detected. While in MGIP algorithm, X_{pl} is the phase information of training sample X_l and a real number, so the covariance matrix $\hat{R}_{pL}$ estimated by X_{pl} will not be affected by the bearing and intensity of the interference target. Therefore, the MGIP algorithm will not nullify in this bearing of interference target, which makes it more sensitive to interfering target with different bearing and intensity. Simulation results demonstrate the validity of this improved method.
2) In the GIP algorithm, the computation of complex matrix inversion $\hat{R}_L^{-1}$ is time consuming, but the MGIP algorithm only needs to compute the real matrix inversion $\hat{R}_{pL}^{-1}$, which reduces the computational burden.

4. THE INTERFERENCE TARGET DETECTION ALGORITHM PERFORMANCE ANALYSIS

There are two hypotheses before our analyzing the algorithm performance. One is that $\hat{R}_L$ is converged (according to [20], if L is large enough, it can be thought true in engineering application); the other is that the moving target is not correlated to the clutter (referring to [11, 21], it can be thought so when considering the moving target average effect on different range cells). Because the clutter echoes are random variable, one range cell clutter echo is only once realization of them; the NHD result based on them is a variable too. So it is not comprehensive to judge an algorithm performance only by the interference targets recognizing results for special range cells. Moreover, the quantitative analysis using these methods is difficult. Therefore, another method from the statistical point of view is proposed to judge an algorithm performance. Referring to paper [22], a sensitive factor of interference target is quoted as follows

$$\alpha_{\mathrm{NHD}} = \frac{E\left[\eta_{\mathrm{NHD}}\left(X_l, \hat{R}_L\right) | \sigma_{it0} > 0\right]}{E\left[\eta_{\mathrm{NHD}}\left(X_l, \hat{R}_L\right) | \sigma_{it0} = 0\right]} = \frac{E\left[\eta_{\mathrm{NHD}}\left(X_{lH} + \sigma_{it0} S_{it0}, \hat{R}_L\right)\right]}{E\left[\eta_{\mathrm{NHD}}\left(X_{lH}, \hat{R}_L\right)\right]} \tag{14}$$

where, S_{it0} is steering vector of interference target being detected in detection cell, and σ_{it0}^2 denotes its power. X_{lH} is a homogenous clutter

part of X_l. $E(^\circ)$ denotes an average value under several range cells. $\eta_{\mathrm{NHD}}(^\circ)\,|\sigma_{it0} > 0$ denotes the NHD output for snapshot X_l containing outlier, while the $\mathrm{NHD}(^\circ)\,|\sigma_{it0} = 0$ denotes for snapshot X_l without outlier. α_{NHD} reflects the algorithm's sensitivity to interference target. The greater is the α_{NHD}, the more evident is the difference between X_l containing and not containing outlier, and the better is the NHD performance.

Substituting the expression (11) into (14) we can get the sensitivity coefficient of GIP

$$\begin{aligned}\alpha_{\mathrm{GIP}} &= \frac{E\left[\eta_{\mathrm{GIP}}\left(X_l, \hat{R}_L\right)|\sigma_{it0} > 0\right]}{E\left[\eta_{\mathrm{GIP}}\left(X_l, \hat{R}_L\right)|\sigma_{it0} = 0\right]} \\ &= \frac{\mathrm{trace}\left[\hat{R}_L^{-1/2}\left(R_l + \sigma_{it0}^2 S_{it0} S_{it0}^H\right)\hat{R}_L^{-1/2}\right]}{\mathrm{trace}\left[\hat{R}_L^{-1/2} R_l \hat{R}_L^{-1/2}\right]}\end{aligned} \tag{15}$$

Substituting the expression (13) into (14) we can get the sensitivity coefficient of MGIP

$$\begin{aligned}\alpha_{\mathrm{MGIP}} &= \frac{E\left[\eta_{\mathrm{MGIP}}\left(X_l, \hat{R}_{pL}\right)|\sigma_{it0} > 0\right]}{E\left[\eta_{\mathrm{MGIP}}\left(X_l, \hat{R}_{pL}\right)|\sigma_{it0} = 0\right]} \\ &= \frac{\mathrm{trace}\left[\hat{R}_{pL}^{-1/2}\left(R_l + \sigma_{it0}^2 S_{it0} S_{it0}^H\right)\hat{R}_{pL}^{-1/2}\right]}{\mathrm{trace}\left[\hat{R}_{pL}^{-1/2} R_l \hat{R}_{pL}^{-1/2}\right]}\end{aligned} \tag{16}$$

5. SIMULATION RESULTS AND ANALYSIS

The performances of proposed algorithm detecting target under non-homogeneous environment are verified through Monte Carlo experiment. The following results are all obtained by averaging 200 times independent experiment values. The airborne radar is side looking, and the main simulation parameters are listed in Table 1.

5.1. The Sensitive Coefficient Simulation under $\hat{R}_L$ Corrupted and Not Corrupted by Interference Target

The NHD aims at distinguishing the contaminated samples by interference target from training samples. In the following simulations, under $\hat{R}_L$ corrupted by interference target, one interference target with parameters SINR = 30 dB, $\theta = 90^\circ$, $2f_d/f_r = 0.25$ was injected into

training samples. From the Equations (15) and (16), it is clear that the sensitive coefficient varied according to intensity, azimuth and Doppler frequency of interference target being detected in detection cell. Its simulation results according to these parameters are shown in Figures 4–6. In these figures, the curve labeled "clean" is the simulation result for $\hat{R}_L$ being not corrupted by interference target, and the curve labeled "dirty" is the simulation result for $\hat{R}_L$ being corrupted by strong one.

Figure 4 shows the variety of α_{GIP} and α_{MGIP} according to detecting interference target intensity. Figure 4(a) shows that, under

Table 1. Parameters for simulation.

Parameter	Value
λ (wavelength)	0.23 m
V (aircraft velocity)	140 m/s
H (aircraft altitude)	8 km
N (number of array channels)	10
K (number of pulses)	12
f_r (pulse repetition frequency)	2435 Hz
d (element spacing)	0.5λ
CNR (clutter-to-noise ratio)	50 dB
$2f_{d0}/f_r$ (target normalized doppler)	0.25
θ (azimuth angle)	90°

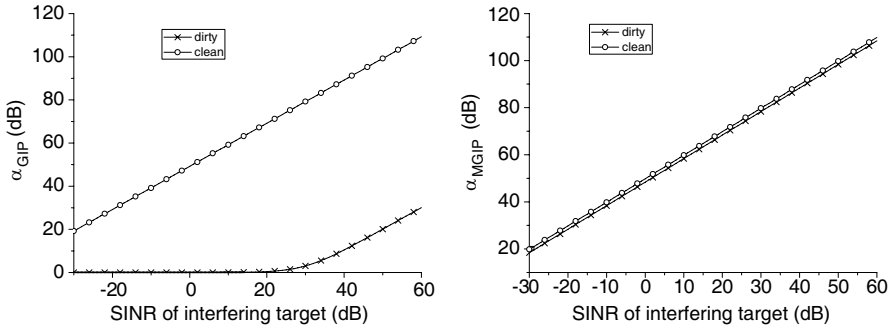

(a) GIP (b) MGIP

Figure 4. The sensitive coefficient versus intensity of interference target in detecting cell.

$\hat{R}_L$ corrupted by strong interference target environment, when the detecting interference target power SINR $< 30\,\mathrm{dB}$, the GIP sensitive coefficient $\alpha_{\mathrm{GIP}} \approx 0\,\mathrm{dB}$ and the outlier cannot be detected. Figure 4(b) shows that MGIP sensitive coefficient is not affected by interference target in training samples.

Figure 5 shows the variety of α_{GIP} and α_{MGIP} according to azimuth of interference target in detecting cell, its other parameters are set at $\mathrm{SINR}_0 = 15\,\mathrm{dB}$, $2f_{d0}/f_r = 0.25$. Figure 5(a) shows that GIP nullifies not only in the direction of clutter but also in the direction of interference target in training data. However, Figure 5(b) shows that MGIP only nullifies in the direction of clutter and is not affected by the interference target azimuth in training data.

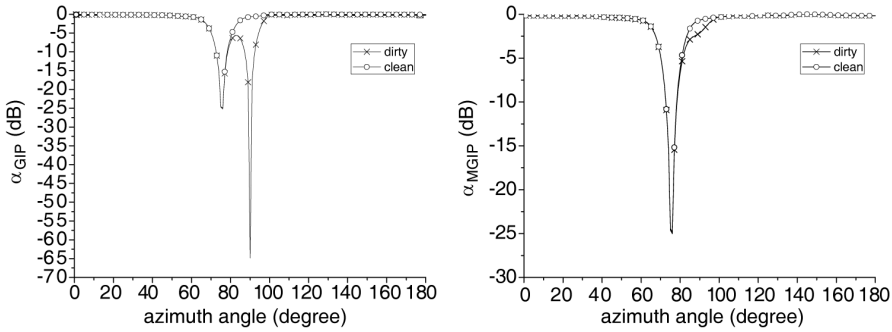

(a) GIP (b) MGIP

Figure 5. The sensitive coefficient versus azimuth of interference target in detecting cell.

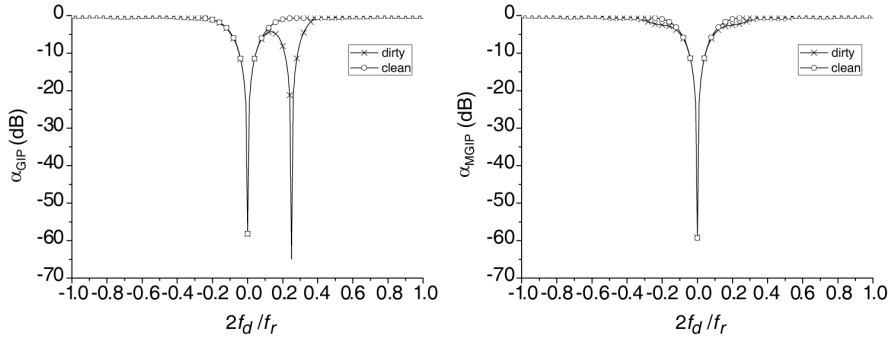

(a) GIP (b) MGIP

Figure 6. The sensitive coefficient versus Doppler frequency of interference Target in detecting cell

Figure 6 shows the variety of α_{GIP} and α_{MGIP} according to Doppler frequency of interference target in detecting cell. Its other parameters are set at $\mathrm{SINR}_0 = 15\,\mathrm{dB}$, $\theta_0 = 90^\circ$. Figure 6(a) shows that GIP nullifies not only in the clutter Doppler frequency but also in the Doppler frequency of interference target in training data. However, Figure 6(b) shows that MGIP only nullifies in the clutter Doppler frequency and is not affected by the interference target Doppler frequency in training data.

Therefore, from Figures 4–6, we can see that the interference targets existing in training samples will reduce the GIP sensitive coefficient at these targets bearing and degrade its interference target reorganization performance. MGIP algorithm is not affected by the interference targets in training snapshots, so it is more robust to recognize them.

5.2. The Performance of Interference Target Detection Algorithm

To verify the performance of interference target detection algorithm, nine outliers are injected into several range cells in a random fashion. In these snapshots, six of them have the form of target-matching space-time steering vector. The cells of existing interference target and the parameters of them are listed in Table 2.

The GIP and MGIP detection results are shown in Figure 7.

In Figure 7(a), only three strong targets lying at cell 50, 75 and 150, and three sidelobe interference targets lying at cell 90, 125 and 175 were detected by GIP; the three weaker ones lying at cell 100, 170 and 200 cannot be detected. Moreover, the interference targets intensity cannot be distinguished. From Figure 7(b) we can see that MGIP detected nine targets clearly, and the intensity of them can be distinguished clearly too.

Table 2. The parameter of interfering target.

Rang cell	50, 75, 150	100, 170, 200	90	125	175
Azimuth	90°	90°	90°	100°	120°
$2f_d/f_r$	0.25	0.25	−0.1	0.25	−0.75
SCNR (dB)	−10	−35	−25	−15	−15

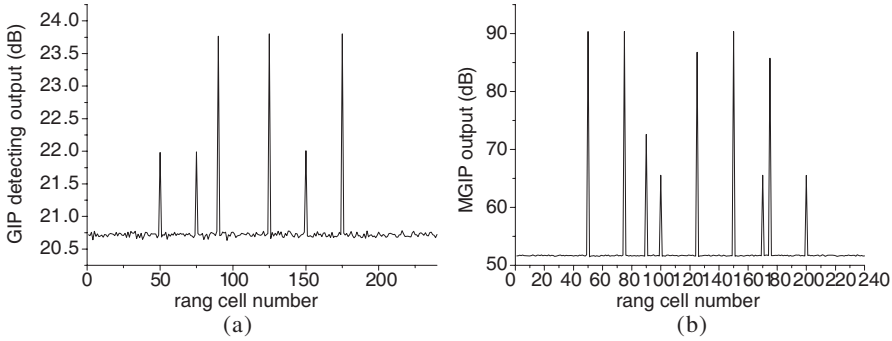

Figure 7. The output test statistic of interfering target detecting algorithm (a) GIP (b) MGIP.

6. CONCLUSION

The presence of interference targets in the secondary data will bias the covariance matrix estimate such that a true target in the primary range cell is suppressed. Therefore, it is important that all relevant interference targets are rejected. Owing to the phase information of the secondary data contains the interference target phase information, the presence of interference targets in the secondary data will lead to their phase nonhomogenous. Moreover, the phase is not affected by the amplitude. Based on these, a new interference targets detection algorithm using the phase information to screen them is proposed. The theoretic analysis and simulations results show that the MGIP algorithm is more robust than the GIP with reduced computation load in detecting the interference targets.

REFERENCES

1. Babayigit, B., K. Guney, and A. Akdagli, "A clonal selection algorithm for array pattern nulling by controlling the positions of selected elements," *Progress In Electromagnetic Research B*, Vol. 6, 257–266, 2008.
2. Rocca, P., L. Manica, and A. Massa, "An effective excitation matching method for the synthesis of optimal compromises between sum and difference patterns in planar arrays," *Progress In Electromagnetics Research B*, Vol. 3, 115–130, 2008.
3. Mahanti, G. K., A. Chakraborty, and S. Das, "Design of fully digital controlled reconfigurable array antennas with fixed

dynamic range ratio," *Journal of Electromagnetic Waves and Applications*, Vol. 21, No. 1, 97–106, 2007.

4. Guney, K. and M. Onay, "Amplitude-only pattern nulling of linear antenna arrays with the use of bees algorithm," *Progress In Electromagnetics Research*, PIER 70, 21–36, 2007.
5. Zhai, Y. W., X. W. Shi, and Y. J. Zhao, "Optimized design of ideal and actual transformer based on improved micro-genetic algorithm," *Journal of Electromagnetic Waves and Applications*, Vol. 21, 1761–1771, 2007.
6. Chen, T. B., Y. L. Dong, Y. C. Jiao, et al., "Synthesis of circular antenna array using crossed particle swarm optimization algorithm," *Journal of Electromagnetic Waves and Applications*, Vol. 20, 1785–1795, 2006.
7. Mouhamadou, M., P. Vaudon, and M. Rammal, "Smart antenna array patterns synthesis: Null steering and multi-user beamforming by phase control," *Progress In Electromagnetics Research*, PIER 60, 95–106, 2006.
8. Qu, Y., G. Liao, S.-Q. Zhu, and X.-Y. Liu, "Pattern synthesis of planar antenna array via convex optimization for airborne forward looking radar," *Progress In Electromagnetics Research*, PIER 84, 1–10, 2008.
9. Ward, J., "Space-time adaptive processing for airborne radar," Technical report 1015, Lincoln Laboratory, MIT, 1994.
10. Aissa, B., M. Barkat, B. Atrouz, et al., "An adaptive reduced rank stap selection with staggered prf, effect of array dimensionality," *Progress In Electromagnetics Research C*, Vol. 6, 37–52, 2009.
11. Melvin, W. L. and M. C. Wicks, "Improving practical space-time adaptive radar," *Proceedings of 1997 IEEE National Radar Conference*, 48–53, Syracuse, New York, 1997.
12. Little, M. O. and W. P. Berry, "Real-time multichannel airborne radar measurements," *Proceedings of 1997 IEEE National Radar Conference*, 138–142, Syracuse, New York, 1997.
13. Adve, R. S., T. B. Hale, and M. C. Wicks, "Transform domain localized processing using measured steering vectors and non-homogeneity detection," *Proceedings of the IEEE National Radar Conference*, 285–290, Boston, MA, April 1999.
14. Wang, Y. L., et al., "Robust space-time adaptive processing for airborne radar in nonhomogeneous clutter environments," *IEEE Transactions on Aerospace and Electronic Systems*, Vol. 39, No. 1, 71–81, January 2003.
15. Gerlach, K. and M. L. Picciolo, "Robust STAP using reiterative

censoring," *Proceedings of the IEEE National Radar Conference*, 244–251, Huntsville, AL, May 5–8, 2003.

16. Gerlach, K., S. D. Blunt, and M. L. Picciolo, "Robust adaptive matched filtering using the FRACTA algorithm," *IEEE Transactions on Aerospace and Electronic Systems*, Vol. 40, No. 3, 929–945, 2004.
17. Blun, S. D., K. Gerlach, and M. Rangaswamy, "STAP using knowledge-aided covariance estimation and the FRACTA algorithm," *IEEE Transactions on Aerospace and Electronic Systems*, Vol. 42, No. 3, 1043–1057, 2006.
18. Shackelford, A. K., K. Gerlach, and S. D. Blunt, "Partially adaptive STAP using the FRACTA algorithm," *IEEE Transactions on Aerospace and Electronic Systems*, Vol. 45, No. 1, 58–69, 2009.
19. Gerlach, K., "Outlier resistant adaptive matched filtering," *IEEE Transactions on Aerospace and Electronic Systems*, Vol. 38, No. 3, 885–901, 2002.
20. Reed, I. S., J. Mallet, and L. Brennan, "Rapid convergence rate in adaptive arrays," *IEEE Transactions on Aerospace and Electronic Systems*, Vol. 10, No. 6, 853–863, 1974.
21. Melvin, W. L. and J. R. Guerci, "Adaptive detection in dense target environment," *Proceedings of the 2001 IEEE Radar Conference*, 187–192, 2001.
22. Dong, R. J., "Study of nonhomogeneous STAP and its application to airborne radar," PhD. thesis, Xidian University, China, 2000.